

# 粒子加速用プラズマフォーカス装置における電極形状のプラズマ流及び電流値への影響評価

## INFLUENCE OF ELECTRODE GEOMETRY ON THE BEAM CURRENT IN A PLASMA FOCUS DEVICE FOR PARTICLE ACCELERATION

ウルデリコ スパダベッキヤ<sup>#, A)</sup>, 志村 尚彦<sup>\*A)</sup>, 柿沼 啓太<sup>B)</sup>, 志熊 良樹<sup>B)</sup>,  
高橋 一匡<sup>B)</sup>, 佐々木 徹<sup>B)</sup>, 菊池 崇志<sup>B)</sup>  
Ulderico Spadavecchia<sup>#, A)</sup>, Naohiko Shimura<sup>A), \*</sup>, Keita Kakinuma<sup>B)</sup>,  
Yoshiki Shikuma<sup>B)</sup>, Kazumasa Takahashi<sup>B)</sup>, Toru Sasaki<sup>B)</sup>, Takashi Kikuchi<sup>B)</sup>  
<sup>A)</sup> Toshiba Energy Systems & Solutions Corporation  
<sup>B)</sup> Nagaoka University of Technology

### Abstract

Experiments on a compact plasma focus device (PFD) have been carried out in order to understand the accelerating mechanisms caused by the interaction of a supersonic plasma with an external magnetic field in a collisionless environment. The present study evaluates the effects of the inner electrode geometry of the PFD on the plasma flow and the resulting beam current.

### 1. Introduction

There is an increased necessity towards more compact and high energy output particle accelerators specially in health care and diverse industrial applications. Inspired in the accelerating mechanisms of high energy particles in cosmic rays [1], in a previous work, experiments on a compact plasma focus device (PFD) were conducted for studying the interactions between fast plasma flows (~30km/s) with magnetic fields in a non-collision environment, for the understanding of the accelerating mechanisms in collisionless shocks, as a candidate for a new particle accelerating method [2-4].

The present work aims analyze the effects of the electrode geometry on the plasma flow and beam current under the presence of an external magnetic field.

### 2. Experimental setup

The experimental setup is shown in Fig. 1. The plasma

focus device is placed inside a vacuum chamber operating at 0.1Pa with Helium gas. A pre-ionization system is placed upstream the PFD electrodes. The system is composed by a coaxial channel made of an insulating material, and a coil connected to an RF source is placed around the chamber in order to induced a plasma as in an induced coupled plasma (ICP) system. The pre-ionization system is placed outside the vacuum chamber in order to avoid plasma from being generated in the surroundings of the coils. The input energy is applied by means of a capacitor bank of 12 $\mu$ F (2 $\mu$ F x 6), charged by a negative power supply up to 15kV. The capacitor bank is connected to the electrodes of the plasma focus device through gap switch operating under self-breaking mode. For this work, two types of inner electrodes were used as shown in Fig. 2. The large electrode (labeled as d) has a total length of 50mm with a cylindrical base of 30mm, and the shorter electrode (labeled as c) has a total length of 40mm with a cylindrical base of 20mm.

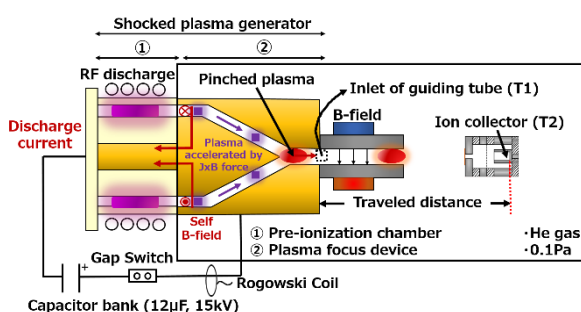


Figure 1: Schematic view of the experimental setup.

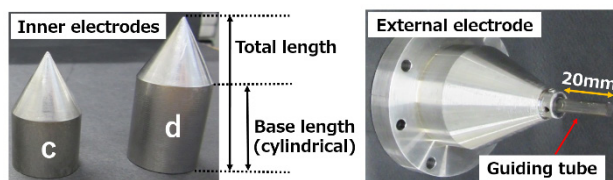


Figure 2: Inner electrodes of the PFD.

As shown in Fig. 2, an acrylic guiding tube is placed downstream the PFD, for the plasma to expand and interact with a perpendicular external magnetic field applied by permanent magnets (not shown in the Fig. 2). The effects of the position of the magnetic field were evaluated by analyzing three different locations (inlet, center, and outlet of the guiding tube) of the permanent magnets (25mT) in the guiding tube, as shown in Fig. 3.

# uldericoclaudioant1.spadavecchia@toshiba.co.jp

\*Present affiliation: Toshiba Environmental Solutions Corporation



Figure 3: Inner electrodes of the PFD.

The typical discharge current has an oscillatory behavior typical of an underdamped system, with a maximum peak current of 70kA, with characteristic frequency  $\omega_L = 4.84 \cdot 10^5 \text{ rad/s}$ . The stray inductance and resistance were estimated by fitting the discharge current with the ideal waveform, using the least squares method, and with a value of 430nH and 18m $\Omega$ , respectively. The discharge current in the present experiment was measured by placing a Rogowski coil as shown in Fig. 1, and the beam current was measured by a Faraday cup placed downstream the guiding tube with a biased voltage of -50V.

### 3. Results and discussions

#### 3.1 Plasma velocity and beam characteristics without external magnetic field

Plasma velocity, discharge and beam currents were evaluated by means of a Faraday cup, where the plasma velocity was estimated using the Time-Of-Flight (TOF) method as shown in Fig. 4.

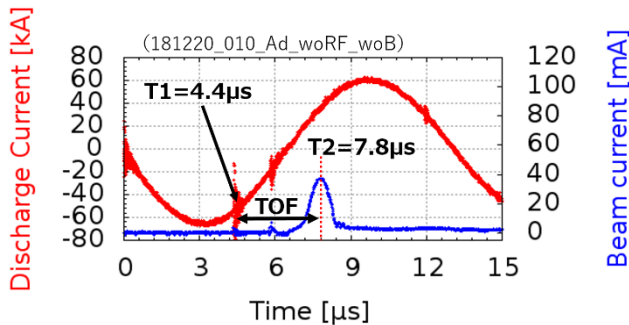


Figure 4: Measurement of parameters.

In Fig. 4, the disturbance in the discharge current at  $T1=4.4\mu\text{sec}$  corresponds to the moment in time where the plasma reaches the tip of the inner electrode and pinches due to the constricting effects of the radial Lorentz force. For the present work it was assumed that the time scales from the plasma pinching and the time it takes the plasma to reach the inlet of the guiding tube, can be neglected and considered as a one instantaneous event. Under this assumption,  $T1$  in Fig. 4 and Fig. 1 are considered to be the same point. On the other hand, point  $T2$  corresponds to the time of arrival of the particles to the Faraday cup. As can be seen in Fig. 4, in the present work  $T2$  was chosen as the moment in which the beam current reaches its peak. And with these times defined, plasma velocity was estimated by Eq. (1) as shown below.

$$v = \frac{\text{Traveled distance}}{T1-T2} = 23\text{km/s} \quad (1)$$

The velocity distribution of both electrodes without and with pre-ionization system are shown in Fig. 5 and Fig. 6, respectively.

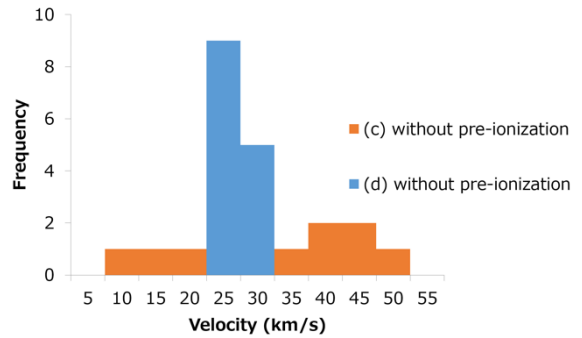


Figure 5: Velocity distribution without pre-ionization.

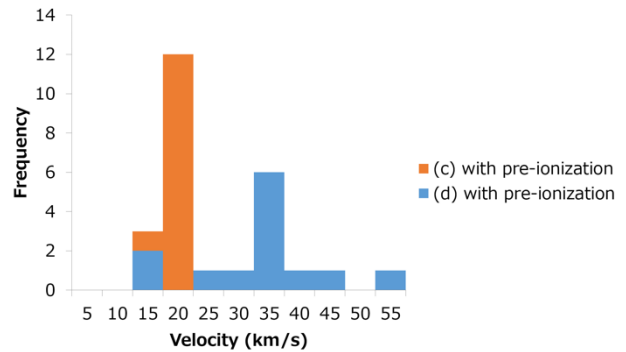


Figure 6: Velocity distribution with pre-ionization.

Without pre-ionization, it can be seen that c-electrode excels in achieving higher velocities compared to the d-electrode, however, the dispersion in the results of the c-electrode is considerably higher than that of the d-electrode.

For the c-electrode, higher velocities are achieved with some dispersion in the results, as can be noted in Fig. 5. The d-electrode on the other hand, did not reach velocities as high as the c-electrode, but excels in terms of reproducibility.

In the case of the c-electrode, higher velocities are achieved when proper conditions are met for the discharge to occur at the base of the electrode (temperature, surface roughness, etc.), allowing a more efficient use of the magneto-hydrodynamic forces along the length of the electrode. The dispersion in the results is attributed by the fact that the discharge starting point is most likely to change in every shot.

For the d-electrode, the lower velocities can be explained by considering that the discharge is most likely to be localized at the tip of the electrode, which is in close proximity with the external tapered electrode. On the other hand, as the discharge is localized to the same point, reproducibility is considerably higher compared to c-electrode.

The above analysis can be further elaborated by noticing that under the present taper PFD geometry, the inter-

electrode area is wider for case of the c-electrode. This means that under the operating conditions of the device at pressures near 0.1Pa, where the breakdown phenomenon corresponds to that in the left side of the Paschen curve, the discharge is most likely to happen at different locations and as more available discharge paths can be possible under a wider space.

When the plasma focus operates with pre-ionization, the opposite effect is observed. For the shorter c-electrode, reproducibility improved but the average achievable velocity decreased from 37.3km/s to 16.4km/s. For the d-electrode, higher velocities were achieved in contrast to the case without pre-ionization, but the dispersion increased.

For the c-electrode case, it was stated above that a wider inter-electrode area increases the possible discharge paths under the current working pressures. Depending on how the free charges from the pre-ionization chamber enter into the inter-electrode area, a preferred discharge point is favored. Based on low velocities achieved, the preferred discharge point is most likely to be closer to the tip of the electrode.

For the d-electrode, the higher velocities are likely to occur when seed charges entering the PFD region, favor the discharge to occur near the base of the electrode. The higher dispersion is explained by considering that the conditions inside the PFD electrode are most likely changing with each shot, favoring at times the discharge initiation at the tip of the electrode. Regardless of this effect, introducing seed charges in the system helps the PFD to initiate discharge away from the tip, and with further improvements of the pre-ionization system, a more efficient use of the PFD at lower pressures can be achieved.

Additionally, studies on the field distribution in the inter-electrode area are also paramount in order to understand further the discharge process. These studies and further improvement of the pre-ionization system under low pressures are to be carried out in future works.

As for the discharge and beam current, typical waveforms are shown in Fig. 7.

The discharge current in red, is characterized by a disturbance that ranges between 3 $\mu$ s and 6 $\mu$ s depending on the case. This disturbance is thought to be produced by both the discharge and the plasma being pinched at the tip. Both effects are thought to be together as the time scales between the discharge and the acceleration towards the tip

of the electrode as most likely in the nano-seconds order. Regarding the beam current, two types of patterns can be seen. In one pattern, the current is composed of only one peak (or one signal), while the second pattern is composed by two peaks, as can be seen in Fig. 7. For instance, for the c-electrode without pre-ionization, of 15 shots, 94% of beam current profiles had two peaks. On the other hand, for the case of d-electrode, 93% of beam current profiles had only one peak.

For the c-electrode case, a possible explanation of the two peaks nature of the beam current, is that some of the insulating material from the pre-ionization chamber in direct contact with the plasma focus electrode, is being ablated during the main discharge and mixed with the Helium plasma. As a consequence, the first peak or signal detected in the beam current corresponds to the source plasma accelerated and the second peak may correspond to those ablated particles coming from the back.

For the d-electrode, a dominating presence of single peaks in the beam current is observed. Based on the previous descriptions, discharges the tip of the d-electrode is less likely to have any effects on the ablation of the insulating material from the pre-ionization chamber. As a consequence, the beam current has predominantly single peaks.

When the pre-ionization system is introduced, the d-electrode showed a 13% increase of double peaks. As previously explained, the presence of seed charges improves the conditions for the discharge to begin near the base of the electrode (or its vicinities), which is the area closest to pre-ionization system.

### 3.2 Plasma velocity and beam characteristics with external magnetic field

The velocity histograms for c and d-electrodes in the presence of a pre-ionization system and an external B-field placed in the guiding tube, are shown in Fig. 8 and Fig. 9, respectively.

In terms of reproducibility, the long d-electrode improved its reproducibility when magnetic field was present. It was observed that the best reproducibility is achieved when the external magnetic field is placed at the outlet of the guiding tube, but average velocity tends to decrease. Furthermore, assuming that in the d-electrode case most of the times the discharge occurs near the tip of the electrode, the farther the magnetic field (outlet of guiding tube), the better the reproducibility. However, a more rigorous analysis must be conducted with a steadier pre-ionization system in order to verify whether the magnetic field has a stabilization effect on the main discharge.

For the c-electrode case, achievable velocities increased with some changes in reproducibility. In contrast, d-electrode case saw an improvement in reproducibility while a decrease in achievable velocities.

The lower velocities achieved are can be attributed to three main factors. The first one being, owed to the trapping of the magnetic field, discharge is favored in the vicinities of the tip of the electrodes. Although velocity is decreased, reproducibility and stability of the discharge

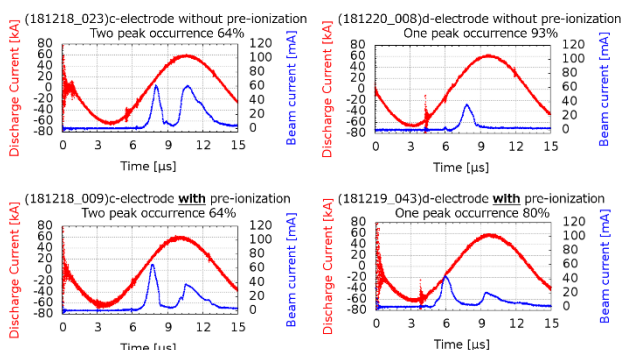


Figure 7: Discharge and beam current characteristics.

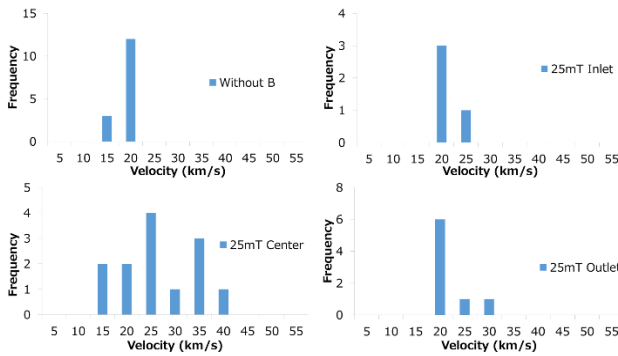


Figure 8: Velocity distributions for “c” electrode.

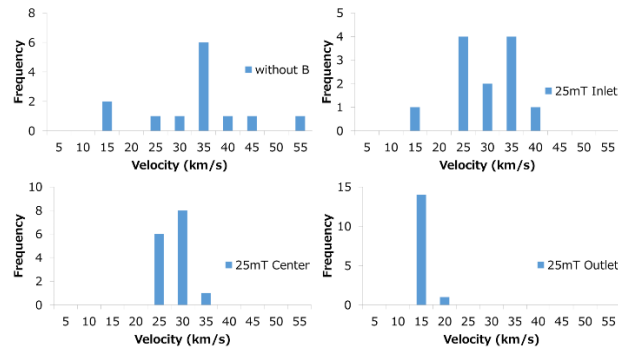


Figure 9: Velocity distributions for “d” electrode.

can be enhanced in the presence of a magnetic. The second factor is the electron motion change by its interaction with the magnetic field, which can give rise to an electrostatic field that affects the motion of ions. The third factor can be attributed to a component of an electric field corresponding to a change in the magnetic due to its interaction with a fast plasma flow. In reference 5, the behavior of a one-dimensional fast plasma flow in a perpendicular magnetic field for understanding the particle acceleration mechanism of collisionless shocks, was investigated numerically. Numerical results show that magnetic field is compressed by the propagation of a fast plasma. The spatial gradient corresponding to this compression, gives rise to an electron motion in the perpendicular direction of both the magnetic field and bulk plasma. As a result, an electric field is caused by the Lorentz force generated from the electron flow induced and the magnetic field. This electric field was shown to be the responsible source of both the deceleration of the bulk plasma and acceleration of the faster ions in the initial Maxwell distribution [5].

On the other hand, a decrease of bulk velocity does not imply that particles are not being accelerated to higher velocities by the interaction of the plasma and the magnetic field. Currently the only measurement device being used is the Faraday cup. In order to evidence and confirm the presence of faster particles, should the shockwave acceleration mechanism be successful, additional measurements with a streak camera are required in order to evaluate the plasma velocity profile along the guiding tube, allowing us to have a better perspective of the physical phenomenon. Additionally, particle collision in the surroundings of the Faraday cup can affect the sensitivity

of the measurements for faster particles. Further improvements of the vacuum conditions, in order to reduce collisions in the surroundings of the faraday cup, are also required and led for future works.

For the discharge and beam currents, results are shown in Fig. 10. As previously mentioned above, because collisions are dominant in the system, signs of accelerated particles in the system cannot be evidenced from the current measurements. there will not be any signs of fast particles in the system.

The rate of single or double peaks in the beam current, varied but without a definite pattern, leading to think that the phenomenon is quite sporadic are requires an improvement on the discharging conditions. In the main discharge current nonetheless, a quite defined second disturbance can be seen in most cases, especially in the c-electrode. However, in contrast to the first disturbance, this second one is believed to be local discharge in an arbitrary position inside the plasma focus electrodes. This phenomenon is clearly product of the external field lines entering the inside of the plasma focus device, although the reason remains unknown for the moment.

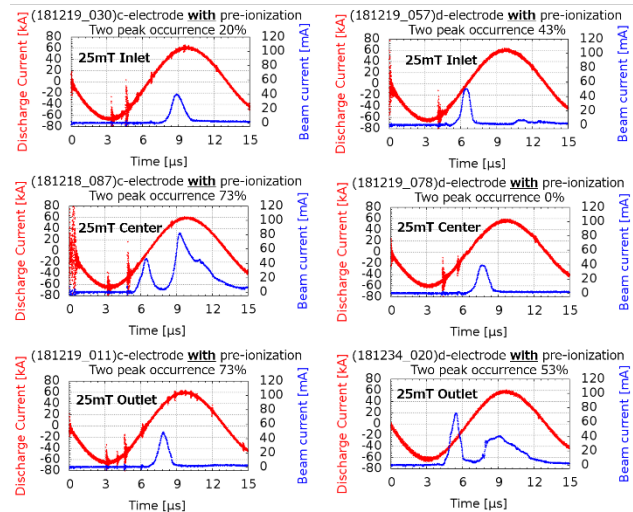


Figure 10: Discharge and beam current characteristics.

#### 4. Concluding remarks

- Performance of a PFD was evaluated under two different inner electrodes under the presence of an external magnetic field. Three different positions of the magnets along the interaction guiding tube were evaluated. Plasma velocity and beam current were the parameters used for evaluation.
- The pre-ionization system effects were confirmed for both electrode cases. Although reproducibility suffered from the non-uniform distribution of seed charges provided by the pre-ionization chamber, velocities higher than the 40km/s were achieved. Further improvement of the pre-ionization chamber under low pressures (0.1~0.5Pa) is required for a more stable seed/plasma production.
- The longer electrode provided a slower plasma

velocity but a more stable operation due to its localized discharge towards the tip of the electrode. With a shorter electrode on the other hand, higher velocities are achieved but reproducibility was affected by the fact that the discharge starting point is most likely to change in every shot due to lower pressure conditions, surface roughness and complex geometrical structure of the taper PFD. The higher velocities in the shorter electrode are thought to originate when the proper conditions for a discharge to happen at the base of the electrode are satisfied. When this occurs, the acceleration process occurs along (almost) the entire length of the electrode, providing a more efficient use of the magneto-hydrodynamic forces.

- Analysis of the effects of external magnetic field was conducted. A more stable operation was evidenced, owe to the trapping effects of the magnetic field lines during the discharge. A decrease of average bulk plasma velocity suggested that: 1) a more localized discharge was enhanced towards the tip of the electrodes, reducing the effective acceleration area along the inner electrode. 2) The magnetic field tends to modify the motion of electrons, which gives rise to an electrostatic electric field that affects the ion motion. 3) An electric field is induced by the compression of the magnetic field due to its interaction with a fast plasma, which tends to decelerate the main bulk plasma. According to numerical results as shown in reference 5, the same induced electric field is also responsible for the acceleration of faster ions in the initial Maxwell distribution.
- Improvement in the vacuum levels downstream the PFD are required for a proper interaction between the plasma and the magnetic field. Furthermore, it is thought that currently, collisions dominate downstream the guiding tube, which in turn affect the detection of accelerated particles in the Faraday cup. Future works will include the use of a streak camera in order to evaluate directly the plasma flow inside the guiding tube.

## References

- [1] M. Hoshino, T. Amano *et al.*, “Particle Acceleration at Shock Waves in the Universe”, The Physical Society of Japan, Vol. 64, No. 6, 2009, pp.412-429.
- [2] U. Spadavecchia, N. Shimura, T. Sako, T. Takezaki, K. Kakinuma, Y. Shikuma, K. Takahashi, T. Sasaki, T. Kikuchi *et al.*, “Influence of an external magnetic field on the velocity profile and beam current in a plasma focus device for particle acceleration”, Proceedings of the 15<sup>th</sup> Annual Meeting of Particle Accelerator Society of Japan, Nagaoka, Japan, Aug. 7-10, pp. 873-876.
- [3] U. Spadavecchia, N. Shimura, T. Takezaki, Y. Hatakeyama, K. Kakinuma, K. Takahashi, T. Sasaki, T. Kikuchi *et al.*, “Experimental study of electrode configuration on the performance of a plasma focus device for particle acceleration”, Proceedings of the Joint Technical Meeting on

“Electrical Discharges” and “Plasma Pulsed Power”, IEE Japan, ED-18-23, PPP-18-5, 2018, pp. 19-23.

- [4] T. Takezaki, K. Takahashi, T. Sasaki, T. Kikuchi, N. Harada *et al.*, “Accelerated ions from pulsed-power-driven fast plasma flow in perpendicular magnetic field”, Physics of Plasma **23**, 2016, 062904.
- [5] T. Takezaki, K. Kakinuma, Y. Shikuma, K. Takahashi, T. Sasaki, T. Kikuchi, N. Harada *et al.*, “Particle acceleration mechanism due to interaction between one-dimensional fast plasma flow and perpendicular magnetic field”, High Energy Density Physics **33**, 2019, 100698.